



TITLE:

Dielectric Relaxation and the Molecular Motion of Poly(vinylidene fluoride)Crystal Form II under High Pressure( Dissertation\_全文)

AUTHOR(S):

Miyamoto, Yoshihisa

---

CITATION:

Miyamoto, Yoshihisa. Dielectric Relaxation and the Molecular Motion of Poly(vinylidene fluoride)Crystal Form II under High Pressure. 京都大学, 1983, 理学博士

ISSUE DATE:

1983-07-23

URL:

<https://doi.org/10.14989/doctor.k2973>

RIGHT:



新制
理
441
京大附図

# 学位申請論文

宮本嘉久



# 学 位 審 査 報 告

氏 名	宮 本 嘉 久
学 位 の 種 類	理 学 博 士
学 位 記 番 号	理 博 第 号
学 位 授 与 の 日 付	昭 和 年 月 日
学 位 授 与 の 要 件	学 位 規 則 第 5 条 第 1 項 該 当
研 究 科 ・ 専 攻	理 学 研 究 科 物 理 学 第 一 専 攻
( 学 位 論 文 題 目 ) $\epsilon$ Dielectric Relaxation and the Molecular Motion of Poly(vinylidene Fluoride) Crystal Form II under High Pressure (ポリフッ化ビニリデンII型結晶の高圧力下における誘電緩和と分子運動)	
論 文 調 査 委 員	主 査 浅 井 健 次 郎 端 恒 夫 中 井 祥 夫

理 学 研 究 科

## (論文内容の要旨)

ポリ弗化ビニリデン (P V D F) は試料処理条件に応じ、種々の多形を示し、特に平面ジグザグに近い分子形態 (conformation) をとる I 型は、高分子で初めての強誘電体として注目されている。この物質の最も安定な結晶型と考えられるものは、 $TGT\bar{G}$  の conformation をとる II 型結晶であるが、この場合結晶の繰返し単位の持つ双極子能率は、分子鎖の長軸に平行、及び垂直な二つの成分を持つ。然し固相での誘電分極に寄与するのは、II 型結晶の場合、その平行成分のみであり、従ってこの分極をもたらす分子運動は、これまで通常考えられていた分子鎖まわりの回転、或いは振動のモードではなく、分子鎖に沿っての conformation の変化 ( $TGT\bar{G} \rightarrow \bar{G}TGT$ ) の移動という、全く新しいモデルによって説明可能であることが、申請者等の論文において提唱されていた。然しその詳細については未だ結論を出すに至っていなかった。

本論文はこの経過をうけて、高圧下での II 型結晶の誘電分散を測定し、その分散機構を明らかにしたものである。この場合試料に高圧を加えることにより、結晶の融点が増加するため、広い温度範囲に亘って、分散強度 (分極の大きさに対応するもの) の温度・圧力効果を調べることができた。この結果明らかになった事実としては、通常の一様な変化とは異なり、分散強度、つまり誘電分極の大きさが、圧力及び温度変化に対し、いずれもある値で極大を与えること、しかもこの時の圧力値  $P_{max}(T)$  及び温度値  $T_{max}(P)$  が、それぞれ温度或は圧力の増加と共に高圧、高温側へ直線的にシフトしてゆくことである。これは圧力範囲としては  $0 \sim 7 \text{ Kbar}$ 、温度としては室温から  $200^\circ\text{C}$  までの、高分子としては相当高温までの温度範囲について測定可能となった結果である。

しかしこのように極大を示すカーブの解析は、既存の配向分極の理論で非常に困難であるが、申請者が既に提出したモデルに基き、分子鎖中の

conformation の乱れは温度上昇と共に増加するが、圧力を加えることによって減少するであろうという、妥当な前提に立って分子鎖の有効双極子能率の温度及び圧力による変化を検討した。この場合分極に寄与する双極子の数を  $N$ ，その有効モーメントの大きさを  $\mu$  としたとき、分散強度  $\Delta \epsilon$  は  $N\mu^2$  に比例するが、申請者はこれらの物理量の圧力、温度依存性を考えるに当り二つのモデルについて検討した。

一つは分子鎖に沿っての分極反転が、分子鎖内のある限られた範囲での欠陥の移動によって起るとした場合で、この場合  $\mu$  は略々一定であるに対し、 $N$  が圧力増加に対して減り、温度上昇で増すことになる。今一つは、分極反転は結晶中の分子鎖全長に亘って起り、従って  $N$  は一定であるが、欠陥部を境としてセグメントのモーメントが、上向きから下向き、或いはその逆に変っているため分子鎖全体の有効モーメントは、それらのベクトル和であらわされる結果、分子鎖中の欠陥の数が多くなる程、上向きと下向きの合計の差、つまり有効モーメント  $\mu$  は平均的に小さくなる。即ち  $\mu$  は温度上昇と共に減り、圧力をかけると減るという、前と逆の傾向を示す。この結果  $N\mu^2$  の変化に他の温度因子の効果を併せ考えると、第 2 のモデルが  $\Delta \epsilon$  の温度・圧力依存性をよく説明するという結果が示された。

申請者は以上の結論に基いて、更にセグメントのモーメントが上向きをとるときと下向きをとるときの自由エネルギーの差  $\Delta g$  と、欠陥を作るときのエネルギー  $W$  という二つの物理量を導入し、確率論を用いて分子鎖の有効モーメント、更に  $\Delta \epsilon$  を表わす式を導いた。この過程で実験結果と一致するように定めた熱力学的パラメーターも、他の実験から評価された諸量とよい一致を示し、モデルの妥当性を立証している。

## (論文審査の結果の要旨)

申請者は、既に本論文の先駆となる論文において、P V D F II 型の誘電分散について注目すべき実験を行ない、その機構について極めて **unique** なモデルを示唆したのであるが、本論文はその結果をうけて、P V D F の分子鎖内の分子運動の様式について一つの具体的な描像を提示し、実験結果によって立証した所にその特色がある。

従来、高分子の誘電分散の機構については、古く Debye の配向分極の理論に基礎を置く **Rigid Rotator** モデル、即ち分子鎖セグメントがその長軸のまわりに回転、若しくは振動することによって起るとする考え方が支配的で、逆にこの事から誘電測定が高分子鎖の運動を評価する一方法として確立してきた。

一方、高分子鎖の誘電分極では、このように配向分極、即ち分子鎖の運動による寄与が重視されてきたことから、試料に対する圧力効果は、その分子間相互作用に及ぼす影響という点において、重要な情報を提供する事が期待されるのであるが、これまで高圧下の誘電測定はそれ程多くはなく、更に温度を変えての測定はより少なかった。

前記内容要旨に説明した通り、申請者は本論文において、広い圧力・温度範囲にわたって P V D F II 型結晶の  $\alpha$  分散の測定を行ない、極めて興味ある実験結果を得た上で、この解析を行なうことによって、誘電分散の機構に関し彼が考えていた二つの可能性のうち、その一つが適当であることを結論した。この結果、これまで出されていたモデルとは全く異なった誘電分極の機構が、確かな実験事実を基礎として、分子論的立場で具体的に表現し得たことに本論文の価値がある。

参考論文第 1 及び第 2 は、本論文の先駆となる研究で、特に後者において、定性的にはあるが分子鎖の **conformation** の変化 ( $TGT\bar{G} \rightarrow \bar{G}TGT$ ) を通して、分子鎖軸に平行成分の分極反転の起る可能性を、実

験結果によって示しており、国の内外で高く評価され、この方面の研究に少なからぬ影響を与えたものである。

これらの論文を通して申請者のこの方面における高い研究能力と学識を評価することができる。よって本論文は理学博士の学位論文として価値あるものと判断する。

なお、主論文及び参考論文に報告されている研究業績を中心とし、これに関連した研究分野について試問した結果、合格と認めた。

Dielectric Relaxation and  
the Molecular Motion of Poly(vinylidene Fluoride)  
Crystal Form II under High Pressure

Yoshihisa MIYAMOTO

Department of Physics, Faculty of Science,  
Kyoto University, Kyoto, 606 Japan

Synopsis

The  $\alpha$  dielectric relaxation of poly(vinylidene fluoride) crystal form II is studied under pressure up to 7 kbar at temperatures from 100°C to 200°C. The dielectric increment shows a maximum against pressure at constant temperatures. This behaviour is examined on the basis of the models of molecular motion for the  $\alpha$  relaxation previously proposed; the longitudinal disorders exist in the crystalline chains. The calculations reproduce the experimental results except the pressure coefficient of the dielectric increment. The metastable conformation exists together with the most stable one in one chain and the dipole reversal parallel to the molecular axis occurs throughout a whole chain.



## I. INTRODUCTION

Dielectric relaxations due to the molecular motions of polymer chains constrained in crystalline fields have been analysed mainly by the site model<sup>1)</sup>, which is originally proposed by Hoffman and Pfeiffer for long chain compounds.<sup>2)</sup> But the limitation of the application of the site model to polymeric substances is not still clear. Recently, Boyd et al.<sup>3),4)</sup> showed that neither the Onsager-Kirkwood equation nor the simple site model could explain the temperature dependence of the dielectric increment in polyethylene; it decreases with temperature faster than the reciprocal of the absolute temperature. They argued that this temperature dependence should be due to the defects in the crystalline chains participating in the relaxation process.

In a previous paper<sup>5)</sup>, we ascertained that the  $\alpha$  dielectric relaxation of poly(vinylidene fluoride) (PVDF) involves only the component of dipole moment parallel to the molecular axis and that the defects in the crystalline region play an important role in the relaxation, and proposed two possible models for the dipolar orientation. But the size of the motional unit and the roles of defects are not still clarified.

In the present paper, the ionic contributions in low frequency region are reasonably subtracted by the method recently developed. Then the  $\alpha$  relaxation ~~are~~<sup>is</sup> studied at high pressures over the wider temperature range than under atmospheric pressure; the melting point increases with

pressure. The dielectric increment showed a maximum against pressure at a constant temperature, which is not expected from the simple site model. The molecular motion associated with the  $\alpha$  relaxation is clarified by taking account of the pressure and temperature dependence of the dielectric increment based on the models previously proposed.

## II EXPERIMENTAL

The material used was KF-polymer #1000 supplied by Kureha Chemical Ind. Ltd. The material was melted in vacuum at 220°C and slowly cooled to room temperature. Then the sample was annealed at 160°C for two days in order to avoid the annealing effects during the dielectric measurements.

The crystal form of the sample was determined by wide angle x-ray diffraction to be form II and no orientation was observed. The long period was 150 Å determined by small angle x-ray scattering. The density was 1.797 g/cm<sup>3</sup> at 20°C and the degree of crystallinity  $\chi$ , is estimated at about 0.6 after the data of Nakagawa and Ishida<sup>6)</sup>.

The dielectric measurements were carried out with a transformer bridge (Fujisoku DLB1102A) over the frequency range from 10<sup>2</sup> to 3×10<sup>5</sup> Hz at temperatures from 100 to 200°C and under pressures up to 7 kbar. The change in the long period and the density before and after the dielectric measurements was not detected within the experimental error.

The high pressure cell (Hikari Kikai Ltd.) used for the dielectric measurements is shown in Fig. 1. The pressure transmitting fluid was a silicone oil (Toshiba TSF451) and pressure was measured by a calibrated manganin gauge.

Silver was evaporated onto both surfaces of the sample to form electrodes of  $79.8 \text{ mm}^2$ . The electrodes of evaporated films were so thin as  $1000 \text{ \AA}$  that the size of the electrodes changes with temperature and pressure following that of the sample. Therefore, the number of dipoles participating in the present measurements is unchanged: The constant number of dipoles contributes to dielectric constant in the present case. Corrections for the cell constant were made as follows. The specific volume of the amorphous parts of PVDF in the present temperature and pressure region has not been reported so far. For the temperature dependence of the specific volume of the crystalline parts  $V_c$  and that of the amorphous parts  $V_a$ , the data of Nakagawa and Ishida<sup>6)</sup> are used. The pressure coefficients of  $V_c$  and  $V_a$  are assumed to be independent of temperature and their pressure coefficients are adopted from the data of Tanaka et al.<sup>7)</sup> at  $150^\circ\text{C}$ . The specific volume of the sample  $V_s(t,P)$  at a temperature  $t$  and a pressure  $P$ , is related to  $V_c$  and  $V_a$  by  $V_s = \chi V_c + (1-\chi)V_a$  and then given by

$$V_s(t,0) = 0.555 + 1.86 \times 10^{-4}t + 4 \times 10^{-7}t^2 \quad (1.a)$$

$$V_s(t,P) = V_s(t,0) (1 - 4.00 \times 10^{-2} P + 7.03 \times 10^{-3} P^2 - 5.47 \times 10^{-4} P^3) \quad (1.b)$$

where  $t$  is temperature in Celsius and  $P$  is pressure in kbar. Then the cell constant  $C(t,P)$  is expressed by

$$\frac{C(t,P)}{C_0} = 1 + \frac{1}{3} \frac{V_s(t,P) - V_0}{V_0} \quad (2)$$

where  $C_0$  and  $V_0$  are the cell constant and the specific volume of the sample at room temperature and under atmospheric pressure, respectively. The maximum contribution from the second term in eq.(2) is 0.019.

### III. RESULTS

The frequency dependence of dielectric constant  $\epsilon'$  and dielectric loss  $\epsilon''$  at 180°C at various pressures is shown in Fig. 2. The frequency at the loss maximum continuously decreases with increasing pressure up to 7 kbar; no sudden change in the relaxation mechanism occurs in this pressure range. The increase in  $\epsilon'$  and  $\epsilon''$  at low frequency region is attributed to interfacial polarization and its frequency dependence is given by<sup>8)</sup>

$$\begin{aligned} \epsilon'_i(\omega) &= A \omega^{-m} \cos \frac{\pi}{2} m \\ \epsilon''_i(\omega) &= A \omega^{-m} \sin \frac{\pi}{2} m \end{aligned} \quad (3)$$



where  $\omega$  is angular frequency and  $A$  and  $m$  depend only on temperature and pressure ( $0 \leq m \leq 1$ ). When, taking the data at  $180^\circ\text{C}$  as examples, we put  $m=0.6$  and the values of  $A$  are determined by a trial and error method, the contribution from interfacial polarization can be subtracted from the observed results. The resulting values of  $\epsilon'$  and  $\epsilon''$  which can be regarded as the values of the  $\alpha$  relaxation, are shown in Fig. 3. In this figure, the dielectric constant is nearly constant at low frequency and the dielectric loss curves represent broad peaks typical to polymeric substances. These dielectric constant  $\epsilon'$  and dielectric loss  $\epsilon''$  nearly obey the Cole-Cole's circular law.

When it is assumed that the increase in  $\epsilon'$  and  $\epsilon''$  at low frequency is expressed by eq.(3) at other temperatures and that the resulting  $\epsilon'$  and  $\epsilon''$  obey the Cole-Cole's law, the observed values of  $\epsilon'$  and  $\epsilon''$  are expressed by

$$\epsilon'(\omega) = \epsilon_\infty + \frac{\Delta\epsilon \cos \phi}{(1 + e^{2\beta x} + 2e^{\beta x} \cos \frac{\pi\beta}{2})^{1/2}} + A\omega^{-m} \cos \frac{\pi m}{2} \quad (4)$$

$$\epsilon''(\omega) = \frac{\Delta\epsilon \sin \phi}{(1 + e^{2\beta x} + 2e^{\beta x} \cos \frac{\pi\beta}{2})^{1/2}} + A\omega^{-m} \sin \frac{\pi m}{2}$$

where  $\epsilon_\infty$  is the limiting value of the dielectric constant at high frequency,  $\Delta\epsilon$  is the dielectric increment,  $\beta$  is the Cole-Cole's parameter representing the distribution of

relaxation times,  $x = \ln \omega \tau$  where  $\tau$  is principal relaxation time and

$$\phi = \arctan \frac{e^{\beta x} \sin(\pi\beta/2)}{1 + e^{\beta x} \cos(\pi\beta/2)}$$

By the least square method, the values of these parameters are determined at each temperature and pressure. The dielectric increment and the relaxation time thus obtained are shown in Fig. 4 and Fig. 5. In the present range of temperature and pressure, the values of  $\beta$  are 0.70-0.78 and those of  $m$  are 0.58-0.62, and they do not depend on temperature and pressure significantly.

It is seen from Figure 4 that firstly, the dielectric increment has a clear maximum against pressure above 120°C. Secondly, the pressure at which  $\Delta\epsilon$  reaches a maximum increases with increasing pressure. Thirdly, the peak value of  $\Delta\epsilon$  decreases with temperature. The activation volume can be obtained from Figure 5; it decreases from 30 to 20 cm<sup>3</sup>/mole with increasing temperature and also shows a slight pressure dependence. The activation enthalpy is obtained from a plot of  $\log \tau$  vs  $1/T$  and the activation internal energy is about 23 kcal/mol. These values roughly agree with the results of Sasabe<sup>9)</sup> and Yano<sup>10)</sup>.

#### IV DISCUSSION

As in a previous paper<sup>5)</sup>, the temperature and pressure

dependence of  $\Delta\epsilon$  is examined on the basis of the two-site model. The dielectric increment  $\Delta\epsilon$  is expressed by

$$\Delta\epsilon = \frac{4\pi}{3kT} K \cdot N \cdot \mu^2 \cdot \text{sech}^2\left(\frac{\Delta G}{2kT}\right) \quad (5)$$

where  $k$  is the Boltzmann constant,  $T$  is the absolute temperature,  $N$  is the number of dipoles per cubic centimeter,  $\mu$  is the component of dipole moment parallel to the molecular axis,  $\Delta G$  is the difference in the Gibbs free energy between the two sites and  $K$  is a correction factor including two factors, i.e. the ratio of the internal field to the applied field and the correction factor for taking the value of dipole moment in vacuum. When  $\Delta U$ ,  $\Delta S$  and  $\Delta V$  are the difference in the internal energy, the entropy and the volume between the two sites, respectively,  $\Delta G$  is given by

$$\Delta G = \Delta U - T\Delta S + P\Delta V . \quad (6)$$

As shown in a previous paper, the  $\alpha$  relaxation involves only the polarization parallel to the molecular axis: dipole reversal due to conformation change from  $TGT\bar{G}$  to  $\bar{G}TGT$ . As there is no entropy difference between the two sites due to the conformation,  $\Delta S$  is assumed to be zero by neglecting the difference due to the volume and the vibration in each site. Moreover,  $\Delta U$  and  $\Delta V$  are assumed to be positive and constant in the measured temperature

and pressure range. Then, from eqs.(5 and 6)  $\Delta\epsilon$  will decrease with pressure for isothermal process, though it may have a maximum against temperature for isobaric process.

For the Onsager internal field which is applicable to a spherical molecule, the term K is given by

$$K = [(\epsilon_{\infty} + 2)/3]^2 \cdot 3\epsilon_0/(2\epsilon_0 + \epsilon_{\infty})$$

where  $\epsilon_0$  is the limiting value of dielectric constant at low frequency. It must be examined, however, whether a molecule can be approximated by a sphere or by an ellipsoid in accordance with the model of the molecular motion. In the following discussion, the temperature and pressure dependence of K is neglected.

#### IV-1 Thermodynamics of Dielectrics

In a dielectrically isotropic system, the Gibbs free energy G of the system is considered to be a function of temperature T, pressure P and electric field E. Its total differential can be expressed by a well-known relation,

$$dG = -SdT + VdP - \frac{M}{4\pi} dE \quad (7)$$

where S is the entropy, V, the volume and M, the polarization of the system. For a system that M is proportional to E, the dielectric increment  $\Delta\epsilon$  is given by M/E. From eq.(7), one finds for isobaric and for isothermal process,



$$\left(\frac{\partial S}{\partial (E^2)}\right)_{P,T} = \frac{1}{8\pi} \left(\frac{\partial (\Delta\epsilon)}{\partial T}\right)_{P,E^2} \quad (8-a)$$

and

$$\left(\frac{\partial V}{\partial (E^2)}\right)_{T,P} = - \frac{1}{8\pi} \left(\frac{\partial (\Delta\epsilon)}{\partial P}\right)_{T,E^2} \quad (8-b)$$

From a contour map of  $\Delta\epsilon$  shown in Fig. 6, it is seen that in region A,  $\Delta\epsilon$  increases with increasing temperature and decreasing pressure, while in region B, on the contrary,  $\Delta\epsilon$  decreases with increasing temperature and decreasing pressure. According to eqs. (8 a) and b)), both of the entropy and the volume of the system increase by applying electric field in region A. Therefore, in region A the system is in an ordered state for the orientation and the packing of dipoles, but in region B the system becomes in a disordered state. However, the broken line in Figure 6 separating the regions A and B does not necessarily imply the phase change from "phase A" to "phase B"; as mentioned above, even in the two-site model, which does not have a phase change at all, the sign of  $\partial(\Delta\epsilon)/\partial T$  changes with temperature.

#### IV-2 Dielectric Increment

For simplicity, let us consider the quantity  $T\Delta\epsilon/\chi$  instead of  $\Delta\epsilon/\chi$ . According to the simple two-site model with the definite potential wells where  $N$  and  $\mu$  are constant with temperature and pressure,  $T\Delta\epsilon/\chi$  is a measure

of  $\text{sech}^2(\Delta G/2kT)$  and will increase with temperature and decrease with pressure.

From the experimental results shown in Fig. 4,  $T\Delta\epsilon/\chi$  at the six isotherms versus pressure are plotted in Fig. 7 ( $\chi=0.6$ ). Above  $120^\circ\text{C}$ ,  $T\Delta\epsilon/\chi$  reaches a maximum at pressure  $P_{\text{max}}(T)$ . The pressure  $P_{\text{max}}(T)$  increases with increasing temperature. The peak value of  $T\Delta\epsilon/\chi$  slightly increases with temperature. In isobars at pressure between 1 kbar and 4 kbar,  $T\Delta\epsilon/\chi$  also has a maximum at temperature  $T_{\text{max}}(P)$ , but the accuracy of  $T_{\text{max}}(P)$  is not good because an isobar includes only five points at most. The temperature dependence of  $P_{\text{max}}(T)$  and the pressure dependence of  $T_{\text{max}}(P)$  are shown in Fig. 8. The relations  $P_{\text{max}}(T)$  and  $T_{\text{max}}(P)$  can be regarded as shown by the same straight line whose tangent  $\theta$  is  $0.0378 \text{ kbar/K}$  and which crosses at  $P=0 \text{ kbar}$  and  $T=357 \text{ K}$ .

The experimental results obtained are not consistent with the behaviour predicted by the simple two-site model. We will then analyze these data based on the two models of molecular motion previously proposed<sup>5)</sup>, where  $N$  and/or  $\mu$  depend on temperature and pressure.

Here, brief explanations of the two models are given.  $\text{TGT}\bar{\text{G}}$  conformation (hereafter referred to as up state or up segment) and  $\bar{\text{G}}\text{TGT}$  conformation (down state) are considered to coexist in one chain in a lamella. In model 1, a conformational defect located at the boundary between up segment sequence and down one is activated thermally and moves along the molecular axis. This defect motion causes

the reversal of dipole moment along the molecular axis. In this model the number of dipoles corresponds to that of the defects and the magnitude of dipole moment is determined by the range in which the defects can move. In model 2, the location of the defects in a chain is fixed during the dipole reversal. Though the reversal of dipole moment occurs throughout one chain, the total moment of a chain is a vector sum of the moments of all the segments in a chain because up and down segments are mixed in a chain. Here, one segment corresponds to two monomers whose conformation is  $TGT\bar{G}$  or  $\bar{G}TGT$ .

The defects under consideration are thermally created in a chain and the defect density should increase with increasing temperature and decreasing pressure. Though the molecular motion causing the  $\alpha$  relaxation is also activated thermally, the life time of the defects are considered much longer than the relaxation times of the  $\alpha$  relaxation. In the following discussion the density of defects is assumed to be an equilibrium value at a given temperature and pressure.

In model 1, the dipole moment can be assumed constant, i.e. the range of the defect movement is unaltered against temperature and pressure, but the number of dipoles which is equal to the number of defects increases with increasing temperature and decreasing pressure. Accordingly, the temperature and pressure dependence of  $T\Delta\epsilon/\chi$  cannot be explained by model 1.

In model 2, the number of dipoles, i.e. that of

chains in crystalline lamellae, is constant, while the dipole moment which is proportional to the difference in the number between up segments and down ones per chain, depends on the arrangements of up and down segments in a chain. The arrangements will depend on the energy difference  $\Delta g = \Delta u - T\Delta s + P\Delta v$  between up state (assumed the most stable conformation) and down state (then, metastable one), and on the defect formation energy  $W = U_1 - TS_1 + PV_1$ . Here,  $\Delta g$ ,  $\Delta u$ ,  $\Delta s$  and  $\Delta v$  are the differences in the Gibbs free energy, the internal energy, the entropy and the volume between up and down states and  $W$ ,  $U_1$ ,  $S_1$  and  $V_1$  are the Gibbs free energy, the internal energy, the entropy and the volume for the defect formation, respectively. The difference in the entropy  $\Delta s$  between up (TGT $\bar{G}$ ) and down ( $\bar{G}$ TGT) states is assumed to be zero as in the case of  $\Delta S$ . Moreover, the defects are assumed to be of TT conformation; we can put  $S_1 = 0$ .

As the defects exist at the boundaries between up segments sequence and down segments sequence, the difference in the number between up and down segments per chain becomes smaller as the number of defects increases. Then, the dipole moment  $\mu$  decreases with increasing temperature and decreasing pressure. In the case that the energy difference between the two states  $\Delta g$  is dominant in determining the arrangements, the ratio of the number of down segments to that of up segments is expressed by  $\exp(-\Delta g/kT)$ ; the dipole moment decreases with increasing temperature and decreasing pressure in this case, too.



Both these effects bring the reduction of the dipole moment with increasing temperature and decreasing pressure. Therefore, together with the term  $\text{sech}^2(\Delta G/2kT)$  in eq.(5),  $T\Delta\epsilon/\chi$  may have a maximum both against temperature and pressure in the case of model 2.

Since, in this way the observed maximum in  $T\Delta\epsilon/\chi$  against temperature and pressure is qualitatively explained by model 2, we try to estimate the values of these parameters which give the observed  $P_{\max}(T)$  and  $T_{\max}(P)$ .

Neglecting the size of the defects, we regard the arrangements of the segments in a chain to be described by the simple Markov process with two states; up and down states. When the transition probability matrix is written as

$$P = \begin{pmatrix} 1-p & p \\ q & 1-q \end{pmatrix}, \quad (9)$$

$T\Delta\epsilon/\chi$  is given from eqs.(5 and A-9) (Appendix),

$$\begin{aligned} T\Delta\epsilon/\chi = & \frac{4\pi}{3k} K \cdot N_0 \cdot \mu_0^2 \cdot \text{sech}^2\left(\frac{\Delta G}{2kT}\right) \left\{ N_S \left(\frac{p-q}{p+q}\right)^2 \right. \\ & \left. + \frac{4pq(2-p-q)}{(p+q)^3} - \frac{1}{N_S} \frac{8pq(1-p-q)}{(p+q)^4} (1-(1-p-q)^{N_S}) \right\} \end{aligned} \quad (10)$$

where the dependence of  $\Delta G$  on the arrangements is neglected. In these equations,  $1-p$ ,  $p$ ,  $q$  and  $1-q$  are the transition probabilities for up-up, up-down, down-up and down-down successions, respectively,  $N_0$  is the number of

segments per unit volume ( $9.1 \times 10^{21} \text{ cm}^{-3}$ ),  $\mu_0$  is the component of dipole moment of one segment parallel to the molecular axis (1.85D) and  $N_s$  is the number of segments per chain. From the long period  $150 \text{ \AA}$ , the degree of crystallinity 0.6 and the c-axis dimension of the unit cell  $4.92 \text{ \AA}$ <sup>11</sup>,  $N_s$  is estimated about 20. The distribution of the lamellar thickness is neglected in deriving eq.(10). In the bracket in eq.(10), the first term multiplied by  $N_s$  is square of the average of the difference between the number of up segments and that of down segments per chain and the second term represents the distribution around the average value.

When the defect density is given by the thermal equilibrium value,  $p$  and  $q$  are expressed in terms of  $\Delta g$  and  $W$ , but as there are six parameters to be determined, the following two extreme cases are examined. Case (i): the energy difference  $\Delta g$  between up and down states is small enough to neglect the first term in the last bracket in eq.(10). In this case, from eq.(A-3),  $p$  and  $q$  are given by

$$p = q = \frac{1}{1 + \exp(W/kT)} \quad . \quad (11)$$

Case (ii):  $\Delta g$  is finite and the main contribution in the last bracket in eq.(10) is  $N_s \left( \frac{p-q}{p+q} \right)^2$ . From eq.(A-3),  $p$  and  $q$  are given by

$$p = \frac{1}{1 + \exp(\Delta g/kT)} ; \quad q = \frac{1}{1 + \exp(-\Delta g/kT)} \quad . \quad (12)$$

In case (i), from eqs (10 and 11),  $T\Delta\epsilon/\chi$  is given by

$$T\Delta\epsilon/\chi = \frac{4\pi}{3k} K \cdot N_0 \cdot \mu_0^2 \cdot F(T, P) \quad (13)$$

where

$$F(T, P) \cong \text{sech}^2\left(\frac{\Delta G}{2kT}\right) \left(e^{W/kT} - \frac{e^{2W/kT} - 1}{2N_s}\right) \quad (14)$$

The relations of  $P_{\max}(T)$  and  $T_{\max}(P)$  are obtained by differentiating  $F(T, P)$  with respect to  $P$  and  $T$ , respectively;

$$P_{\max}(T) : \left. \frac{\partial F(T, P)}{\partial P} \right|_{P=P_{\max}} = 0$$

and

$$T_{\max}(P) : \left. \frac{\partial F(T, P)}{\partial T} \right|_{T=T_{\max}} = 0$$

As both the relations  $P_{\max}(T)$  and  $T_{\max}(P)$  give the same linear function in the observed temperature and pressure range, i.e. around  $P=0$  kbar and  $T=T_0=357$  K, the relations between parameters are obtained as follows:

$$V_1/\Delta V = U_1/\Delta U \quad (15)$$

$$\begin{aligned} & \frac{\Delta U}{2kT_0} \tanh\left(\frac{\Delta U}{2kT_0}\right) \\ &= \frac{U_1}{2kT_0} \frac{e^{U_1/kT_0} - e^{2U_1/kT_0}/N_s}{e^{U_1/kT_0} - (e^{2U_1/kT_0} - 1)/N_s} \end{aligned} \quad (16)$$

$$\theta = U_1/T_0 V_1 \quad (17)$$

where  $\theta$  is the tangent of the straight line in Fig. 8. From eqs. (15, 16 and 17), when one of the parameters, for example,  $U_1$  is given, the other parameters i.e.  $V_1$ ,  $\Delta U$  and  $\Delta V$ , can be determined.

In model 2, one dipole corresponds to one chain. Then the value of  $K$  should be calculated for an ellipsoidal molecule with a distribution of dipole moments. If the dipole distribution is replaced by a mathematical dipole at the center,  $K$  can be calculated from the formulae for the internal field and the reaction field of an ellipsoid<sup>12)13)</sup> to be

$$K = \{ 1 + (\epsilon_\infty - 1) A_1 \}^2 \cdot \epsilon_0 / \{ \epsilon_0 + (\epsilon_\infty - \epsilon_0) A_1 \} \quad (18)$$

where

$$A_1 = \frac{abc}{2} \int_0^\infty ds / (s+a^2)^{3/2} (s+b^2)^{1/2} (s+c^2)^{1/2} \quad (19)$$

and  $a$ ,  $b$  and  $c$  are the semi-principal axes of an ellipsoid ( $a > b > c$ ). When an ellipsoid is approximated by a spheroid with the longest major axis given by the lamellar thickness ( $90 \text{ \AA}$ ) and the other two major axes by the unit cell dimensions ( $4.9 \text{ \AA}$  for each), the value of  $K$  ranges from 1.14 to 1.15 for the  $\alpha$  relaxation. The value of  $K$  is taken to be 1.14 in the numerical calculations of  $T\Delta\epsilon/\chi$ .

By fitting the calculated values of  $T\Delta\epsilon/\chi$  to the



experimental ones at  $P_{\max}$ , we obtain the values of parameters as  $\Delta U = 1.5$  kcal/mol,  $\Delta V = 4.4$  cm<sup>3</sup>/mol,  $U_1 = 1.8$  kcal/mol and  $V_1 = 5.4$  cm<sup>3</sup>/mol. The values of  $T\Delta\epsilon/\chi$  calculated from eq.(13) are shown in Fig. 9(a).

In case (ii), from eqs.(10) and (12),  $T\Delta\epsilon/\chi$  is given by

$$T\Delta\epsilon/\chi = \frac{4\pi}{3k} K \cdot N_0 \cdot \mu_0^2 \cdot \text{sech}^2\left(\frac{\Delta G}{2kT}\right) \times \{N_s \tanh^2\left(\frac{\Delta g}{2kT}\right) + \text{sech}^2\left(\frac{\Delta g}{2kT}\right)\} \quad (20)$$

In the same way as case (i), the following relations between parameters are obtained:

$$\Delta V/\Delta U = \Delta v/\Delta u \quad (21)$$

$$\frac{\Delta U}{2kT_0} \tanh\left(\frac{\Delta U}{2kT_0}\right) = \frac{\Delta u}{2kT_0} (N_s - 1) \tanh\left(\frac{\Delta u}{2kT_0}\right) \times \text{sech}^2\left(\frac{\Delta u}{2kT_0}\right) / \{(N_s - 1) \tanh^2\left(\frac{\Delta u}{2kT_0}\right) + 1\} \quad (22)$$

$$\theta = \Delta U/T_0 \Delta V \quad (23)$$

By fitting the calculated values to the experimental ones at  $P_{\max}$ , we obtain the values of parameters as  $\Delta U = 1.3$  kcal/mol,  $\Delta V = 3.9$  cm<sup>3</sup>/mol,  $\Delta u = 0.92$  kcal/mol and  $\Delta v = 2.8$  cm<sup>3</sup>/mol. The calculated results of  $T\Delta\epsilon/\chi$  are shown in Fig. 9(b)

No significant difference is seen in figures 9(a) and

(b). Therefore, we cannot decide which case is preferable for the  $\alpha$  relaxation.

The parameter values obtained are 5-20% of the activation parameters and so they are considered reasonable values. The calculated results explain the experimental ones, but the pressure dependence of  $T\Delta\epsilon/\chi$  is much smaller than the experimental results. The discrepancy may be due to the approximations for deriving eqs.(17 and 22).

We can check the alternatives of these two cases by examining the dependence of  $T\Delta\epsilon/\chi$  on  $N_s$ . Nakagawa and Ishida reported that under atmospheric pressure, the dielectric increment linearly increases with the lamellar thickness but the dielectric increment does not become zero by the linear extrapolation of the lamellar thickness to zero<sup>14)</sup> Their results may indicate that the present two cases coexist in the  $\alpha$  relaxation. If these two cases are mixed, we cannot determine all the parameters by the present method because the data available are insufficient.

Structure analyses recently reported suggest that various disordered structures exist in crystal form II of PVDF<sup>15)16)</sup>, which may justify the present treatments. The dynamical mechanisms of the polarization along the molecular axis are examined by a kink propagation and the activation energy obtained by the calculations agrees with the experimental results<sup>17)</sup>.

## V. CONCLUSIONS

The molecular motion causing the  $\alpha$  relaxation in crystal form II of PVDF is essentially the one that  $TGT\bar{G}$  conformation changes into  $\bar{G}TGT$  one. This molecular motion occurs throughout the chains in crystallites. Since the metastable conformations exist as "defects" together with the most stable ones in a chain, the dipole moment of one chain decreases with increasing temperature and decreasing pressure. As a result, the dielectric increment shows a maximum against pressure and temperature.

## Acknowledgements

The author would like to express his sincere thanks to Professor K. Asai and Dr. H. Miyaji of Kyoto University for helpful advices and encouragements throughout this work. The author also wishes to thank Dr. N. Murayama of Kureha Chemical Ind. Co. Ltd. for supplying the material.

## APPENDIX

When each chain is assumed to be independent and has a different value of dipole moment,  $N\mu^2$  in eq. (5) should be written as

$$\begin{aligned} N\langle\mu^2\rangle &= N \left\langle \sum_{i=1}^{N_s} \mu_i \sum_{j=1}^{N_s} \mu_j \right\rangle \\ &= N(N_s\mu_0^2 + 2\langle \sum_{1 \leq i < j \leq N_s} \mu_i \mu_j \rangle) \end{aligned} \quad (A-1)$$

where  $N_s$  is the number of segments per chain and  $\mu_i$  is the dipole moment of  $i$ -th segment in a chain which equals  $+\mu_0$  or  $-\mu_0$ . We consider the following situations (1) Up state(1-state) of which the segment has a dipole moment of  $+\mu_0$ , is the ground state. (2) Down state(2-state) of which the segment has a dipole moment of  $-\mu_0$ , has a higher energy than up state by  $\Delta g$ . (3) Between the up state sequence and the down state one, a defect should intervene and the defect formation energy  $W$  is necessary.

Under these conditions, we regard the arrangements of the segments in a chain to be described by the simple Markov process. When the transition probability from  $i$ -state to  $j$ -state is written as  $P_{ij}$  ( $i, j=1, 2$ ), from the definition of the probabilities  $\sum_{j=1}^2 P_{ij}=1$ , the probability transition matrix  $P$  can be expressed by

$$P = \begin{pmatrix} 1-p & p \\ q & 1-q \end{pmatrix} \quad (A-2)$$

From the above conditions,  $p$  and  $q$  are given by

$$\frac{p}{1-p} = e^{-(\Delta g + W)/kT} \quad \text{and} \quad \frac{q}{1-q} = e^{-(W - \Delta g)/kT}$$

and hence,

$$p = (1 + e^{(\Delta g + W)/kT})^{-1} \quad \text{and} \quad q = (1 + e^{(W - \Delta g)/kT})^{-1} \quad (\text{A-3})$$

Then from eq. (A-1),  $N\langle\mu^2\rangle$  can be expressed as follows

$$N\langle\mu^2\rangle = N(N_s\mu_0^2 + 2\mu_0^2 \sum_{1 \leq i < j \leq N_s} (\omega_1, \omega_2) P_{UP}^{i,j-i} N_s^{-j} \begin{pmatrix} 1 \\ 1 \end{pmatrix}) \quad (\text{A-4})$$

where the matrix U is given by

$$U = \begin{pmatrix} 1 & 0 \\ 0 & -1 \end{pmatrix} \quad (\text{A-5})$$

and the initial vector  $(\omega_1, \omega_2)$  is assumed to be given by the fractions of up segment and down segment, respectively, that is,

$$\omega_1 = \frac{q}{p+q} \quad \text{and} \quad \omega_2 = \frac{p}{p+q} \quad . \quad (\text{A-6})$$

Since  $P^m$  can be calculated to be

$$P^m = \frac{1}{p+q} \begin{pmatrix} q, p \\ q, p \end{pmatrix} + \frac{(1-p-q)^m}{p+q} \begin{pmatrix} p, -p \\ q, -q \end{pmatrix} \quad , \quad (\text{A-7})$$

the sum in eq. (A-4) is given by

$$\begin{aligned}
\sum_{1 \leq i < j \leq N_s} (\omega_1, \omega_2) p^i u p^{j-i} u p^{N_s-1} \binom{1}{1} &= \frac{1}{2} N_s (N_s - 1) \left( \frac{p-q}{p+q} \right)^2 \\
+ (N_s - 1) \frac{4pq(1-p-q)}{(p+q)^3} - \frac{4pq(1-p-q)^2}{(p+q)^4} (1 - (1-p-q)^{N_s-1}) &\quad (A-8)
\end{aligned}$$

Substituting into (A-4) and from  $NN_s = N_0$ , we obtain

$$\begin{aligned}
N \langle \mu^2 \rangle &= N_0 \mu_0^2 \left\{ N_s \left( \frac{p-q}{p+q} \right)^2 + \frac{4pq(2-p-q)}{(p+q)^3} \right. \\
&\quad \left. - \frac{1}{N_s} \frac{8pq(1-p-q)}{(p+q)^4} (1 - (1-p-q)^{N_s}) \right\} \quad (A-9)
\end{aligned}$$

## REFERENCES

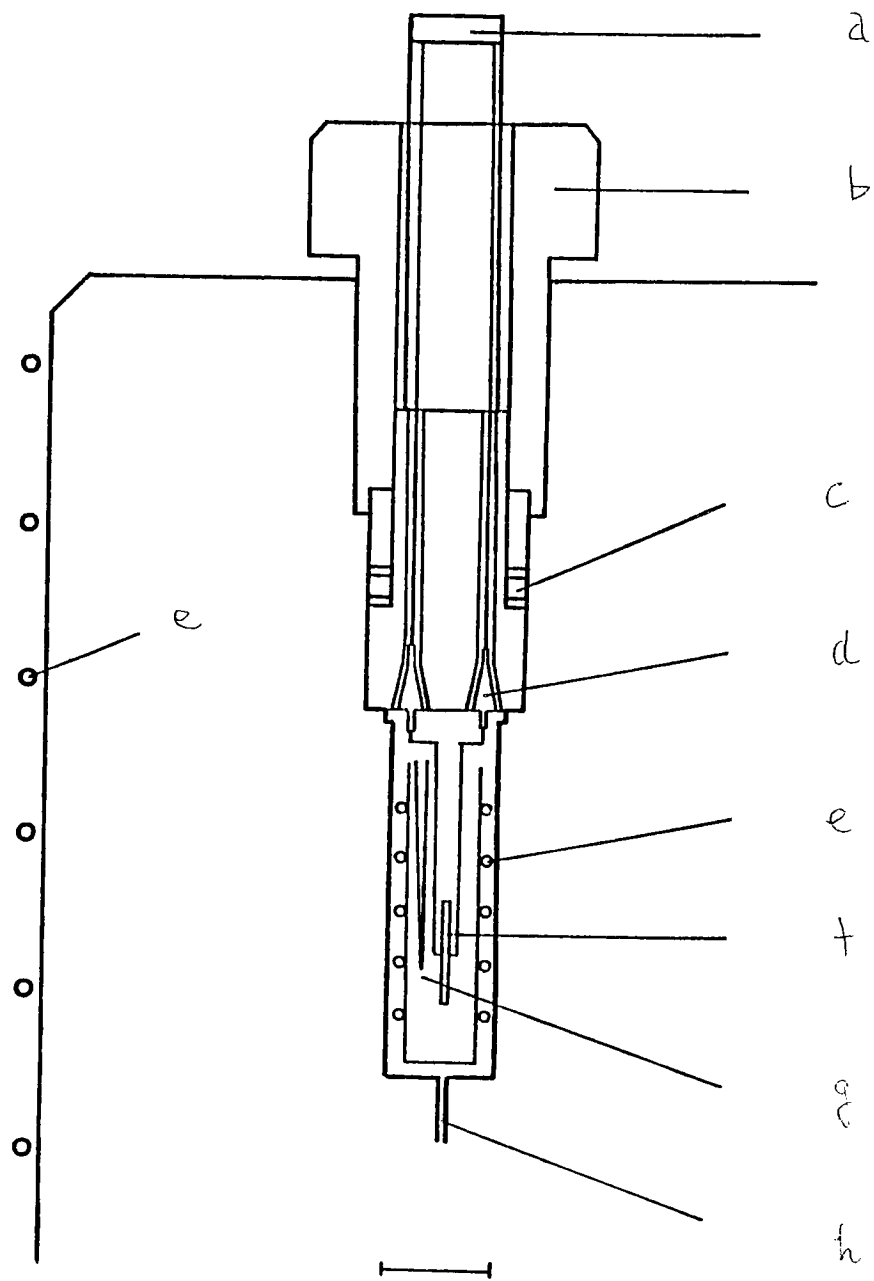
- 1) Hoffman, J. D., Williams, G. and Passaglia, E., J. Polym. Sci. Pt. C 1966, 14, 173
- 2) Hoffman, J. D. and Pfeiffer, H. G., J. Chem. Phys., 1954, 22, 132
- 3) Sayre, J. A., Swanson, S. R. and Boyd, R. H., J. Polym. Sci. Polym. Phys. Ed., 1978, 16, 1739
- 4) Boyd, R. H., and Sayre, J. A., J. Polym. Sci. Polym. Phys. Ed., 1979, 17, 1627
- 5) Miyamoto, Y., Miyaji, H. and Asai, K., J. Polym. Sci. Polym. Phys. Ed., 1980, 18, 579
- 6) Nakagawa, K. and Ishida, Y., Kolloid. Z. z. Polym., 1973, 251, 103
- 7) Tanaka, H., Takayama, K., Okamoto, T. and Takemura, T. Polymer J. 1982, 14, 719
- 8) Yano, S., Tadano, K., Aoki, K. and Koizumi, N., J. Polym. Sci. Polym. Phys. Ed., 1974, 12, 1875
- 9) Sasabe, H., Researches of the Electrotechnical Laboratory, 1971, no.721,
- 10) Yano, S., J. Polym. Sci., Pt.A-2, 1970, 8, 1057
- 11) Hasegawa, R., Takahashi, Y., Chatani, Y. and Tadokoro, H., Polym. J., 1972, 3, 600
- 12) Scholte, Th. G., Physica, 1949. 15, 436
- 13) Böttcher, C. J. F., Theory of Electric Polarization (Elsevier Publishing Company, New York, 1952), Chapter 3

- 14) Nakagawa, K. and Ishida, Y., J. Polym. Sci. Polym. Phys. Ed., 1973, 11, 1503
- 15) Takahashi, Y. and Tadokoro, H., Macromolecules, 1980, 13, 1317
- 16) Bachmann, M. A. and Lando, J. B., Macromolecules, 1981, 14, 40
- 17) Clark, J. D., Taylor, P. L. and Hopfinger, A. J., J. Appl. Phys., 1981, 52, 5903

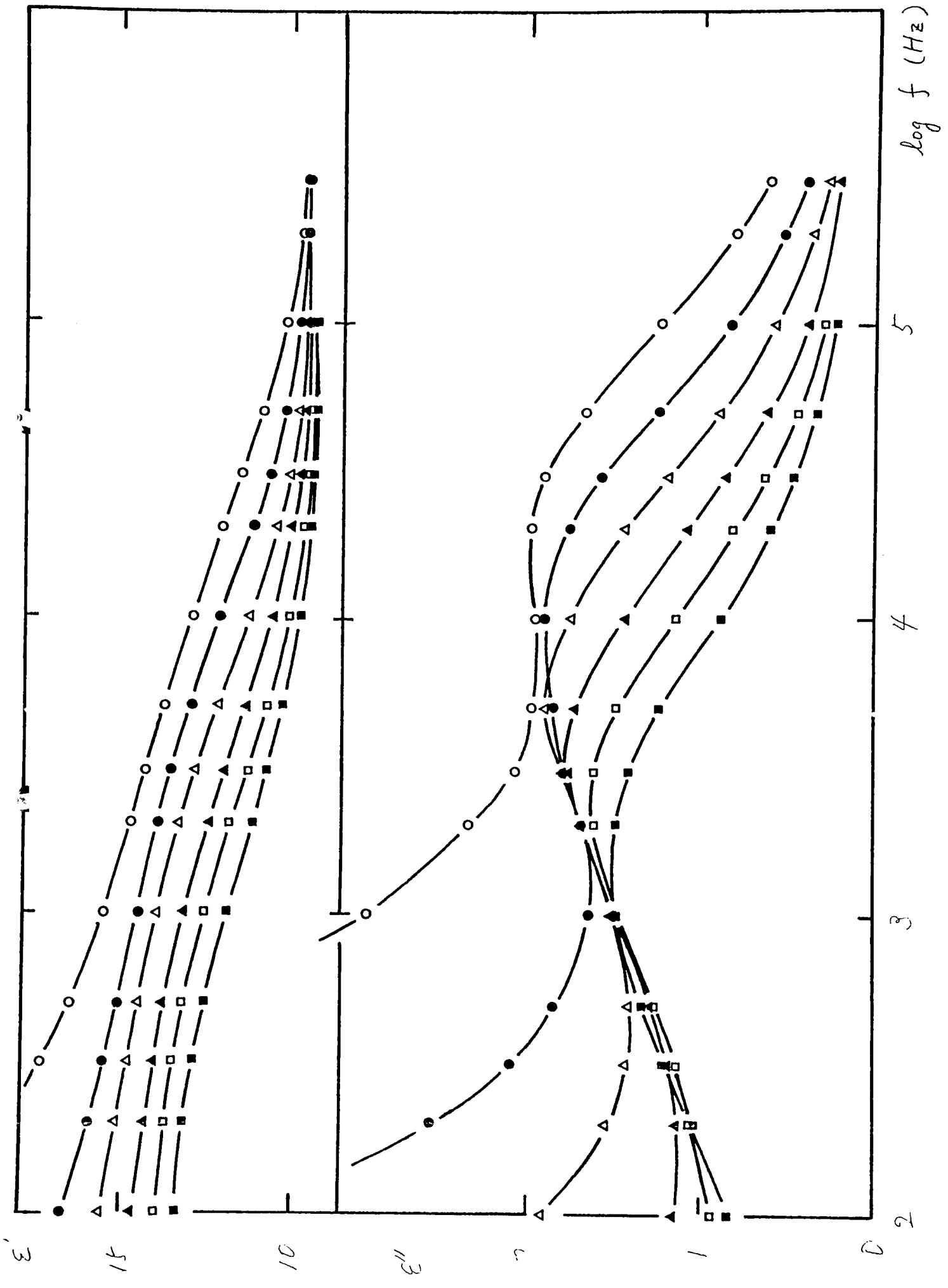


## FIGURE CAPTIONS

- Fig. 1. The high pressure cell for dielectric measurements. a)connector, b)upper end plug, c)packings, d)terminals, e)heater, f)sample, g)thermocouple, h)inlet for oil
- Fig. 2. The frequency dependence of dielectric constant  $\epsilon'$  and loss  $\epsilon''$  at 180°C under various pressures: o; 2.0 kbar, ●; 3.0 kbar,  $\Delta$ ; 4.0 kbar, ▲; 5.0 kbar, □; 6.0 kbar, ■; 7.0 kbar. No correction is made for the cell constant in Figs. 2 and 3.
- Fig. 3. The contribution from the low frequency process(interfacial polarization) is subtracted from the values in Figure 2. The symbols are the same with Fig. 2.
- Fig. 4. The pressure dependence of the dielectric increment at various temperatures:  $\Delta$ ; 100°C, ▲; 120°C, o; 140°C, ●; 160°C, □; 180°C, ■; 200°C.
- Fig. 5. The pressure dependence of relaxation time. The symbols are the same with Fig. 4.
- Fig. 6. Contour map of the dielectric increment.
- Fig. 7. The pressure dependence of  $T\Delta\epsilon/\chi$ . The symbols are the same with Fig. 4.
- Fig. 8. Relations of  $P_{\max}(T)$  and  $T_{\max}(P)$ . Open circles indicate  $P_{\max}(T)$  obtained from Figure 7 and solid ones,  $T_{\max}(P)$ .
- Fig. 9. Calculated results of  $T\Delta\epsilon/\chi$ . a); case (i) and (b); case (ii): 1; 120°C, 2; 160°C, 3; 200°C. Parameter values are given in the text.



20 mm



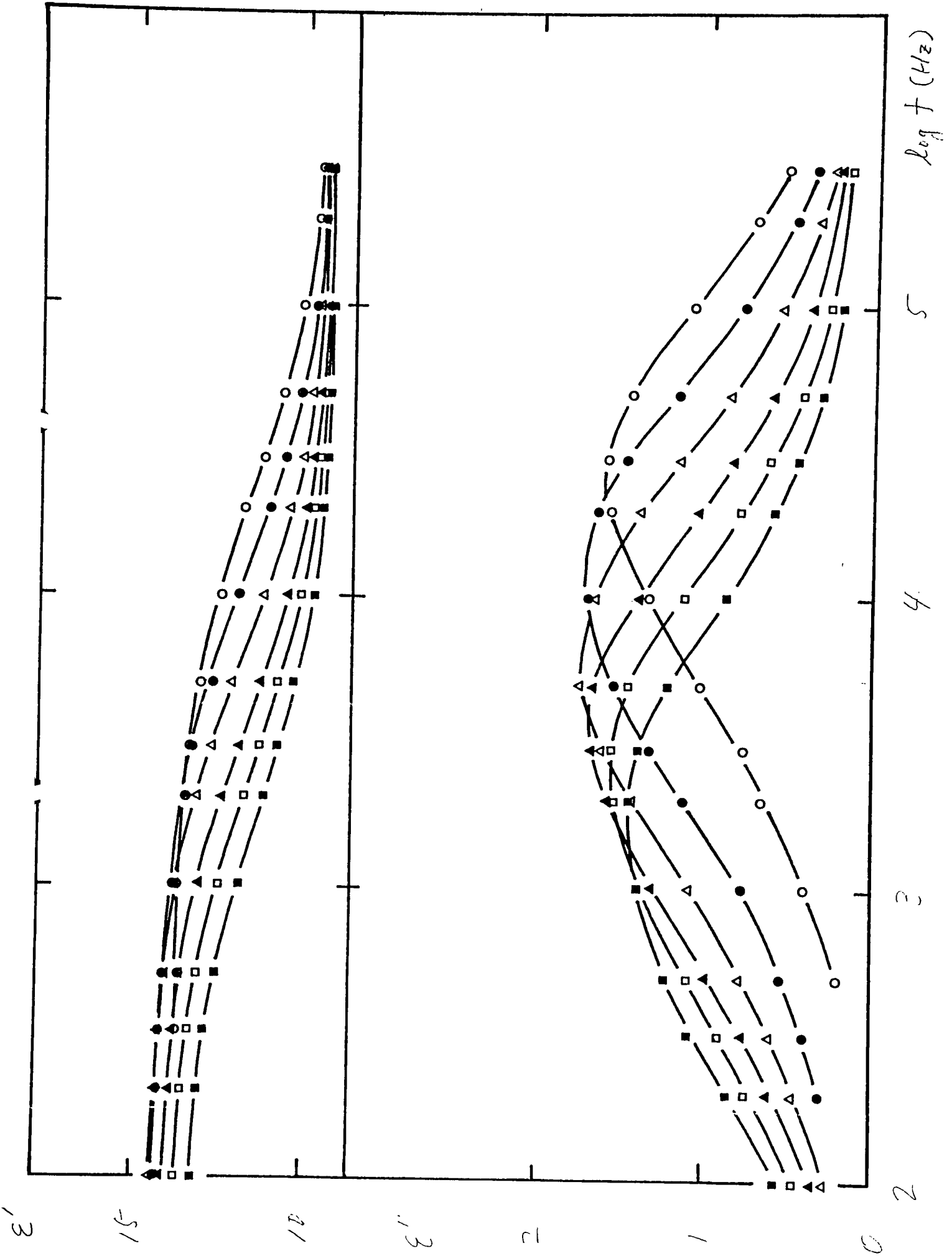


Fig 2

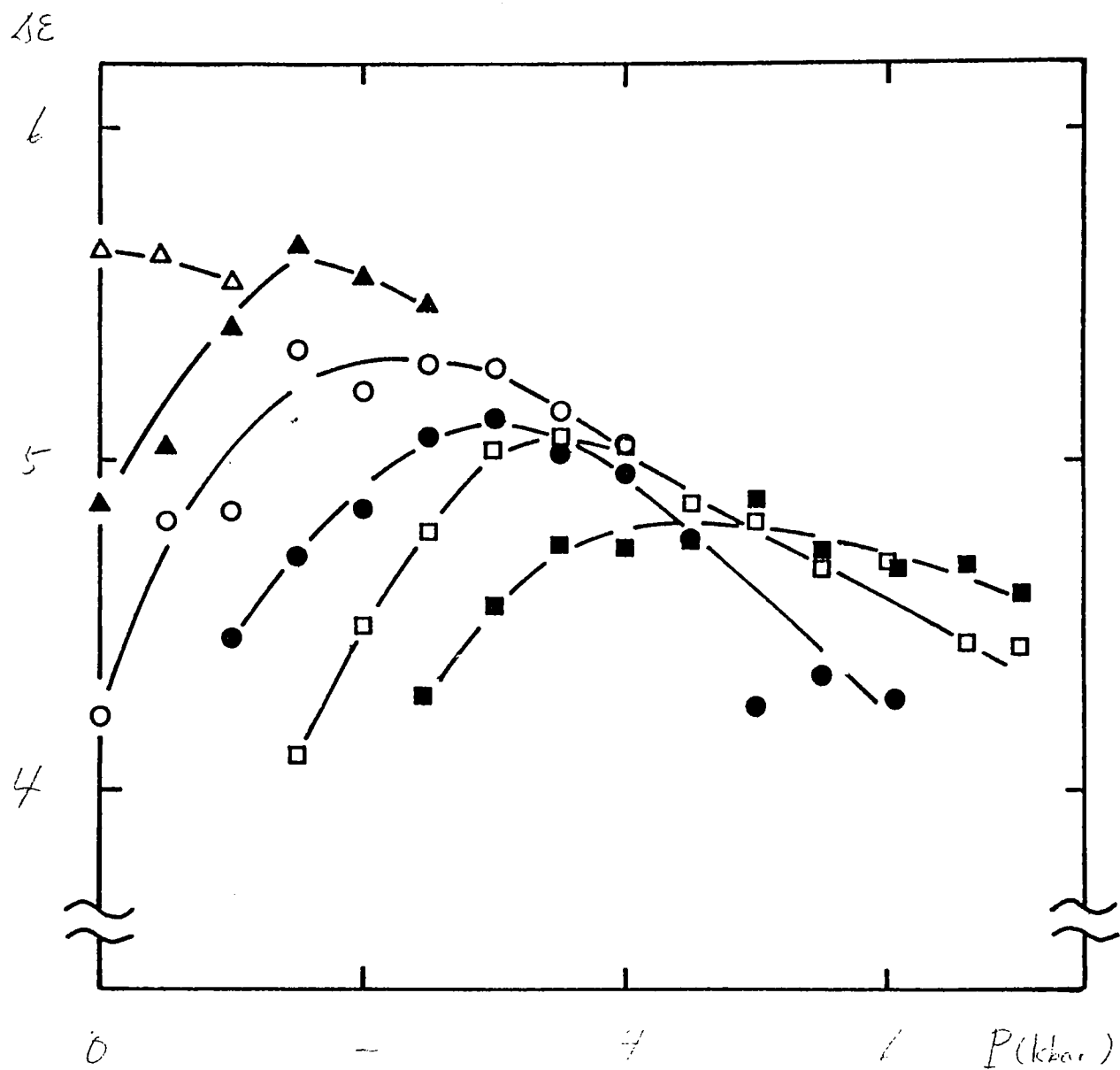


Fig 5

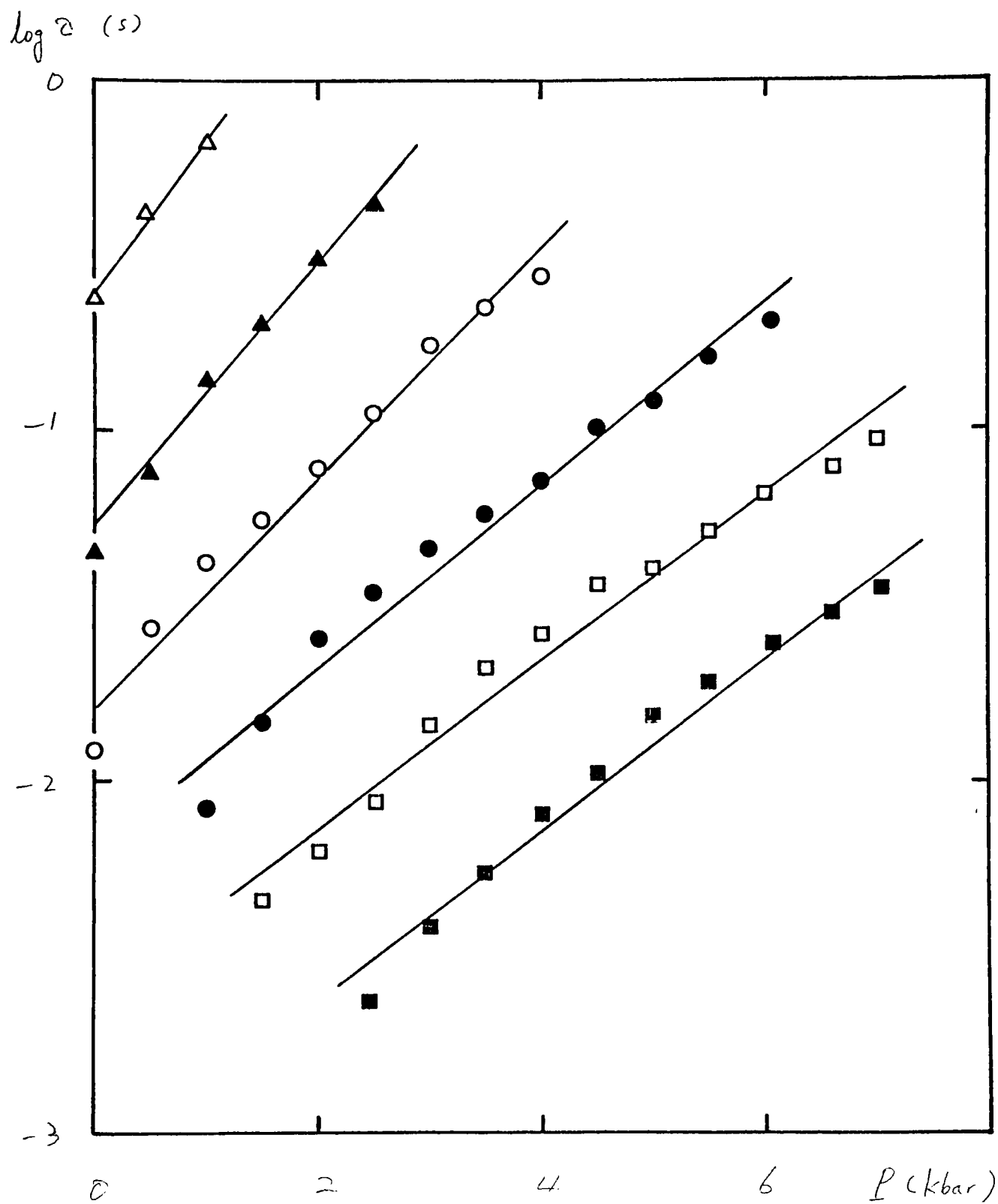
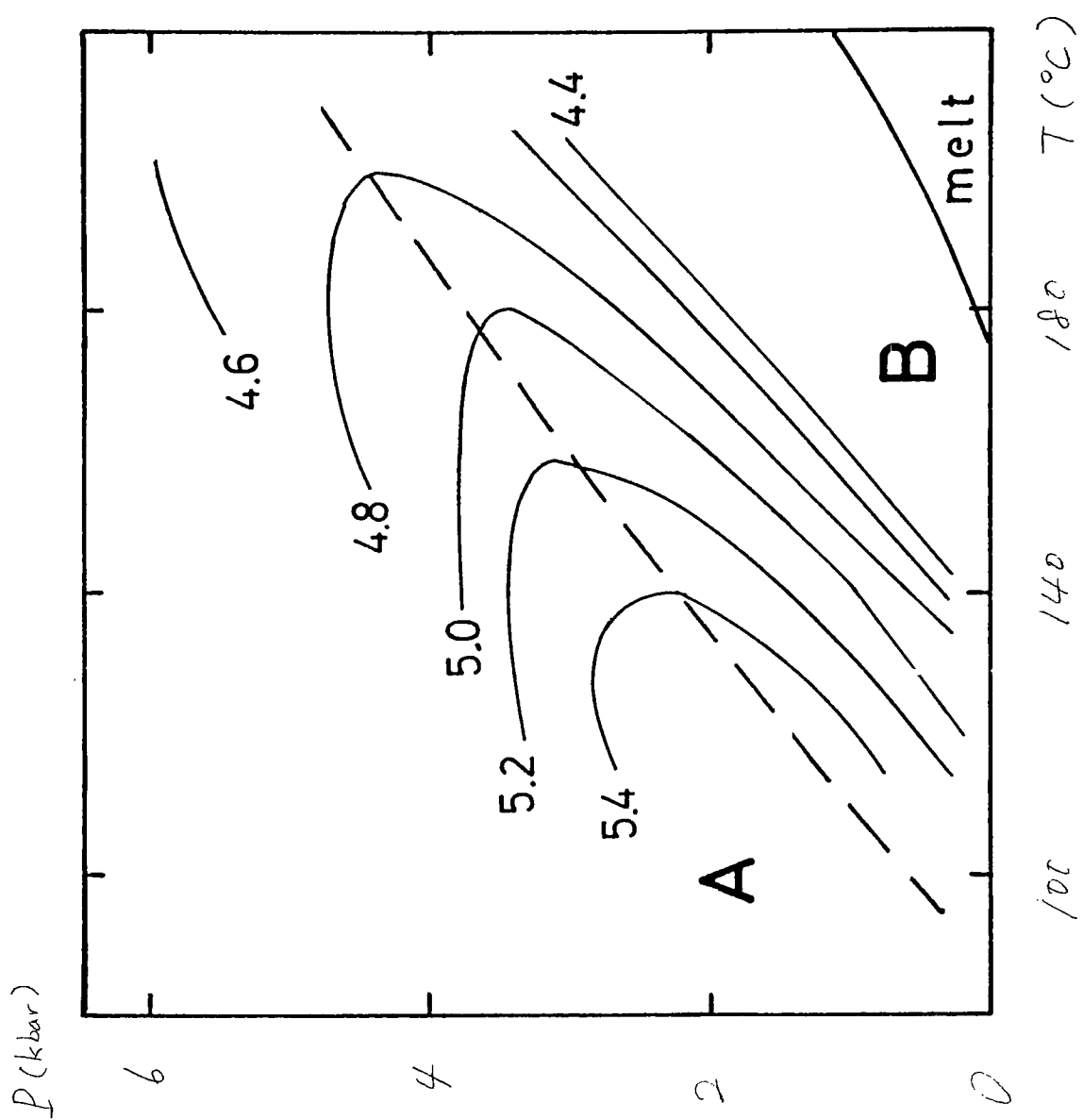


Fig. 6



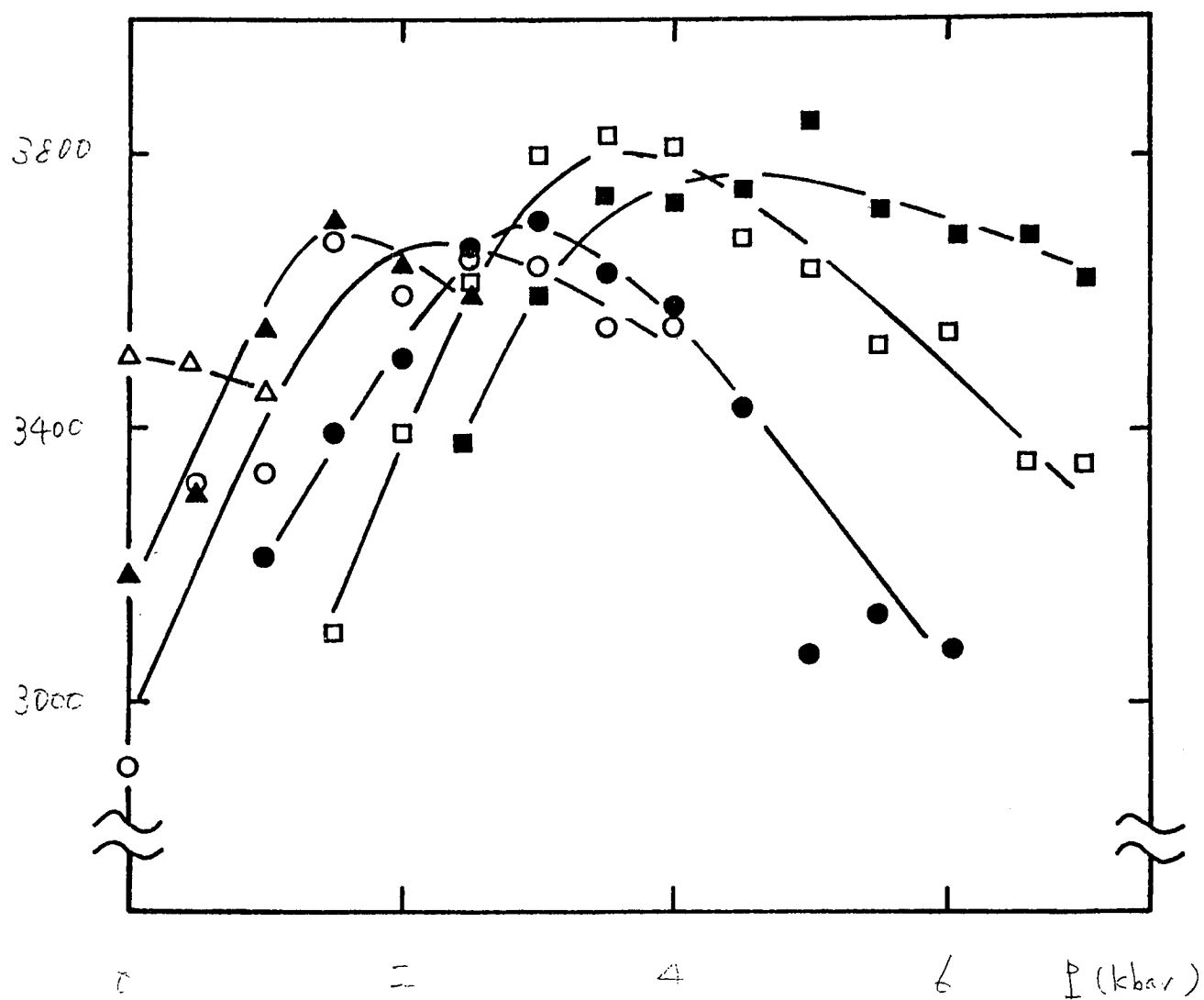
$T_{\Delta E/x} (K)$ 



Fig 8

